Received: 12 April 2023 | Revised: 29 May 2023 | Accepted: 1 June 2023

DOI: 10.1111/jon.13135

JOURNAL OF NEUROIMAGING
THE OFFICIAL JOURNAL OF THE AMERICAN SOCIETY OF NEUROIMAGING
WILEY

CLINICAL INVESTIGATIVE STUDY

Brain FDG-PET findings in chimeric antigen receptor T-cell therapy neurotoxicity for diffuse large B-cell lymphoma

Silvia Morbelli[1,2] | Massimiliano Gambella[3] | Anna Maria Raiola[3] | Chiara Ghiggi[3] | Matteo Bauckneht[1,2] | Tania Di Raimondo[2] | Caterina Lapucci[1,4] | Gianmario Sambuceti[1,2] | Matilde Inglese[1,4] | Emanuele Angelucci[1,3]

[1]IRCCS Ospedale Policlinico San Martino, Genova, Italy

[2]Nuclear Medicine Unit, Department of Health Sciences (DISSAL), University of Genoa, Genova, Italy

[3]Department of Hematology and Cellular Therapy, IRCCS Ospedale Policlinico San Martino, Genova, Italy

[4]Department of Neuroscience, Rehabilitation, Ophthalmology, Genetics, Maternal and Child Health (DINOGMI), IRCCS Ospedale Policlinico San Martino, University of Genoa, Genova, Italy

Correspondence
Matteo Bauckneht, Nuclear Medicine, IRCCS Ospedale Policlinico San Martino, and Department of Health Sciences (DISSAL), University of Genoa, 16132 Genova, Italy.
Email: matteo.bauckneht@hsanmartino.it

Funding information
AIRC, Grant/Award Number: IG 23201

Abstract

Background and Purpose: Chimeric antigen receptor (CAR) T-cell therapy is potentially associated with treatment-related toxicities mainly consisting of cytokine release syndrome (CRS) and immune-effector cell-associated neurotoxicity syndrome (ICANS). We evaluated brain metabolic correlates of CRS with and without ICANS in diffuse large B-cell lymphoma patients treated with CAR-T.

Methods: Twenty-one refractory DLCBLs underwent whole-body and brain [^{18}F]-fluorodeoxyglucose (FDG) PET before and 30 days after treatment with CAR-T. Five patients did not develop inflammatory-related side effects, 11 patients developed CRS, while in 5 patients CRS evolved in ICANS. Baseline and post-CAR-T brain FDG-PET were compared with a local controls dataset to identify hypometabolic patterns both at single-patient and group levels ($p < .05$ after correction for family-wise error [FWE). Metabolic tumor volume (MTV) and total lesion glycolysis (TLG) were computed on baseline FDG-PET and compared between patients' subgroups (*t*-test).

Results: ICANS showed an extended and bilateral hypometabolic pattern mainly involving the orbitofrontal cortex, frontal dorsolateral cortex, and anterior cingulate ($p < .003$ FWE-corrected). CRS without ICANS showed significant hypometabolism in less extended clusters mainly involving bilateral medial and lateral temporal lobes, posterior parietal lobes, anterior cingulate, and cerebellum ($p < .002$ FWE-corrected). When compared, ICANS showed a more prominent hypometabolism in the orbitofrontal and frontal dorsolateral cortex in both hemispheres than CRS ($p < .002$ FWE-corrected). Mean baseline MTV and TLG were significantly higher in ICANS than CRS ($p < .02$).

Conclusions: Patients with ICANS are characterized by a frontolateral hypometabolic signature coherently with the hypothesis of ICANS as a predominant frontal syndrome and with the more prominent susceptibility of frontal lobes to cytokine-induced inflammation.

KEYWORDS
brain PET, CAR-T, lymphoma, neuroinflammation

INTRODUCTION

Chimeric antigen receptor (CAR) T-cell therapy is a promising treatment for refractory or relapsed diffuse large B-cell lymphoma (DLBCL) patients.[1] This novel treatment has shown an early and high response rate and has been associated with an increased overall survival.[1,2] The drawback of this treatment is the potential occurrence of relevant treatment-related toxicities mainly consisting of cytokine release syndrome (CRS) and neurotoxicity, namely, the so-called immune-effector cell-associated neurotoxicity syndrome (ICANS). CRS is a multisystem inflammatory syndrome characterized by fever, hypotension, and hypoxia, potentially leading to multisystem organ dysfunction.[1,3] CRS is very common in patients treated with CAR-T and it is caused by the widespread release of pro-inflammatory cytokines by the activated CAR T cells.[1,4–7]

In some patients, T-cell expansion and associated cytokine production can specifically affect the central nervous system resulting in ICANS. ICANS may occur in up to one third of patients using commercially available CAR-T therapies.[1,8–13]

Pretreatment disease burden, in vivo CAR T-cell expansion, CAR T-cell dose, and severe CRS are considered risk factors for ICANS. Clinical features and time course of ICANS are heterogeneous and may include headache, mild cognitive impairment, language disorders, and other motor deficits, such as seizure and, potentially, global encephalopathy, possibly leading to death.[8–12] Conversely, low-grade neurotoxicity associated with CAR T-cell therapy is typically managed conservatively with supportive care.[1]

The Immune-Effector Cell-Associated Encephalopathy scale, a neurotoxicity grading scale incorporating clinical symptoms, has been proposed for the evaluation of these patients.

To date, there are no specific disease-modifying treatments. High-grade neurotoxicity can be treated with corticosteroids to mitigate the function of CAR T cells and other bystander immune cells that are activated after CAR T-cell infusion.[1,11] Patients' support is also based on symptom management (especially of cerebral edema and seizures), and in case of severe (grade 3-4) neurotoxicity, monitoring in the intensive care unit is required.

ICANS has been associated with a variety of neuroimaging manifestations. Nonetheless, MRI can often be normal or associated with nonspecific findings even in patients with moderate to severe neurotoxicity.[14–16] By contrast, an understanding of the imaging manifestations of ICANS has the potential to increase our comprehension of disease pathophysiology and related risk factors, thus resulting in a potential impact on patients' management. Indeed, while there are no validated models to predict the occurrence of ICANS, fever, high serum interleukin (IL)-6, and high monocyte chemoattractant protein-1 concentrations within the first 36 hours after CAR-T administration have been associated with severe neurotoxicity and could be considered for early identification of patients with ICANS and for their monitoring.

[^{18}F]-Fluorodeoxyglucose (FDG)-PET has a well-recognized role in the staging, restaging, and therapy response assessment in patients with lymphomas including patients candidate for or treated with CAR-T.[17–25]

At present, both in trials and clinical practice, whole-body [^{18}F]FDG PET is performed before and around 30 days after treatment with CAR-T.[1,17–25] Preliminary data have linked the metabolically active tumor burden as measured with PET with the risk of developing CRS.[24–26] In particular, it has been suggested that patients with higher baseline metabolic tumor volume (MTV) may have more severe CRS.[25] Finally in keeping with the well-established role of [^{18}F]FDG PET in patients with neurocognitive disorders, few case reports or small case series have highlighted alterations in brain metabolism in patients with CRS and/or CAR-T neurotoxicity.[9,27–29] However, the vast majority of these case reports are based on visual inspections, and to date no group analyses have been carried out to evaluate metabolic correlates of CRS with or without ICANS. As [^{18}F]FDG PET is routinely performed after treatment with CAR-T, this tool could also be used to further disclose pathophysiological correlates of neurotoxicity related to CAR T cells and, potentially, to early identify risk factors, onset, and resolution of the syndrome.

Given these premises, we aimed to evaluate brain metabolic correlates of CRS with and without ICANS as assessed by [^{18}F]FDG PET acquired 30 days after therapy in DLBCL patients treated with CAR-T. We also aimed to investigate the relationship between PET-assessed baseline MTV and total lesion glycolysis (TLG) on one side and the occurrence of CRS with and without ICANS on the other.

METHODS

Patients

This is an ancillary analysis performed in a subgroup of patients treated with CAR T cells at IRCCS Ospedale Policlinico San Martino for relapsed or refractory DLCBL between October 2020 and November 2022. All patients treated with CAR-T in our center received lymphodepletion (LD) with fludarabine and cyclophosphamide, as per commercial schedule, followed by infusion of axicabtagene ciloleucel or tisagenlecleucel. They all had a whole-body [^{18}F]FDG PET including a dedicated brain acquisition performed at baseline before LD and 30 days after infusion (PET-30). Further inclusion criteria were the presence of measurable nodal disease at baseline on whole-body [^{18}F]FDG PET and the availability of a brain MRI scan performed at baseline as part of a local protocol aiming to exclude other ongoing neurological diseases at baseline. Clinical MRI protocol in our institution included the following sequences: 3-dimensional T1 magnetization-prepared rapid gradient-echo, turbo spin echo T2, 3-dimensional fluid-attenuated inversion recovery (FLAIR), diffusion-weighted imaging with apparent diffusion coefficient, susceptibility-weighted imaging, and T1-weighted contrast-enhanced acquisition. In this framework, nonspecific brain MRI alterations present at baseline and unchanged after CAR T were not considered an exclusion criterion. By contrast, exclusion criteria for the present ancillary analysis were (1) baseline or posttherapy MRI findings suggesting the presence of brain lesions related or unrelated to DLBCL or (2) the presence of cerebral MRI findings suggestive of acute ischemia and hemorrhage and (3)

postradiation brain changes due to previous treatments evident on baseline MRI and/or [^{18}F]FDG PET. The study was approved by the Ethical Committee of Regione Liguria (50/20—DB ID 10306). Patients gave their informed consent, and all procedures and informed consent collection were in accordance with the ethical standards of the 1964 Helsinki Declaration.

Brain and body [^{18}F]FDG PET acquisition and image analysis

Patients underwent both whole body and brain [^{18}F]FDG PET acquisitions according to the European Association of Nuclear Medicine (EANM) guidelines on a Siemens Biograph 16 PET/CT system (the EANM Research Ltd-certified scanner).[30,31]

Brain [^{18}F]FDG PET preprocessing

Image preprocessing was conducted using Statistical Parametric Mapping software version 12 (SPM12; Wellcome Trust Center for Neuroimaging, London, UK).[32] Brain [^{18}F]FDG PET images were spatially normalized using the Montreal Neurological Institute atlas. All the default choices of SPM were followed with the exception of spatial normalization. For this study, the $H_2{}^{15}O$ SPM-default template was replaced by a brain [^{18}F]FDG PET as detailed elsewhere.[33] The spatially normalized set of images was then smoothed with an 8-mm isotropic Gaussian filter to blur individual variations in gyral anatomy and to increase the signal-to-noise ratio.

Whole-body PET analysis

To compute lesions' MTV, a volume of interest was drawn using a standardized uptake value (SUV)-based automated contouring program (Syngovia Siemens workstation, Siemens Medical Solutions, Princeton, NJ, USA) with a volumetric region of interest based on a 3-dimensional isocontour at 41% of the maximum pixel value (SUV_{max}).[34] MTV was obtained by the sum of MTV values of all patients' lesions. TLG was computed as the sum of TLG of every lesion for each patient (thus corresponding for each patient, to the sum of the VOI average/mean SUV value for each lesion multiplied by the corresponding MTV).

Statistical analysis

Patients were subgrouped according to the presence of CRS without ICANS (CRS group), CRS with ICANS (ICANS group), or absence of CAR T-related inflammatory toxicities (no-toxicity). Dedicated brain acquisition of the 3 patients' subgroups acquired at baseline and as part of PET-30 was independently compared with a dataset of normal controls acquired on the same scanner and previously recruited in our laboratory. The original dataset included 48 subjects without any neurologic or psychiatric disease, as detailed elsewhere.[35] Among the 48 normal controls, only 21 subjects belonging to the same age range of patients treated with CAR T were included in the present analysis. To fully explore brain metabolic correlates of CAR T-related toxicities, we also compared posttherapy brain PET of CRS and ICANS

TABLE 1 Patients' characteristics.

Patients	*N* = 21
Age, years (mean ± SD)	55.8 ± 11.8
Sex	
Female	10
Male	11
Histology	
DLBCL NOS	11
DLBCL (tFCL)	6
DLBCL/high grade	2
PMBCL	2
ECOG PS at baseline	
0	12
≥1	9
Bridging therapy	
No	0
Yes	21
Radiotherapy as bridge	
No	11
Yes	10
Bulky (lesion ≥10 cm)	
No	14
Yes	7
Extranodal disease	
No	6
Yes	15
Ferritin levels pre-lymphodepletion	
Normal value	13
High value (>ULN)	8
LDH pre-lymphodepletion	
Normal value	7
High value (>ULN)	14
CRP pre-lymphodepletion	
<5 mg/dL	11
>5 mg/dL	10
CAR T-cell	
Axicabtagene ciloleucel	10
Tisagenlecleucel	11

Abbreviations: CRP, C-reactive protein; DLBCL, diffuse large B cell lymphoma; ECOG PS, Eastern Cooperative Oncology Group Performance Status; LDH, lactate dehydrogenase; *N*, number; NOS, not otherwise specified; PMBCL, Primary Mediastinal B-Cell Lymphoma; SD, standard deviation; tFCL, transformed-follicular cell lymphomas; ULN, upper limit of normal.

TABLE 2 Demographics and disease course in patients with CRS with or without ICANS.

Pt	Age (years), sex	CRS start/end (max grade)	CRS manifestations (maximum grade)	ICANS start/end (maximum grade)	ICANS neurological manifestations	Treatment
1	52, male	Start day 1/end day 6 (max grade 3)	Fever, hypotension (grade 3), hypoxia (grade 2)			Tocilizumab
2	70, female	Start day 3/end day 8 (max grade 2)	Fever, hypotension (grade 2), hypoxia (grade 2)			Tocilizumab
3	68, female	Start day 5/end day 8 (max grade 1)	Fever			None
4	58, male	Start day 3/end day 7 (max grade 1)	Fever			None
5	28, female	Start day 2/end day 7 (max grade 1)	Fever			Tocilizumab
6	68, female	Start day 2/end day 4 (max grade 1)	Fever			Tocilizumab
7	61, male	Start day 1/end day 10 (max Grade 3)	Fever, hypotension (grade 3), hypoxia (grade 2)	Start day 8/end day 9 (max grade 3)	Lethargy (awake on physical stimulation only)	Tocilizumab, Dexamethasone, Anakinra
8	44, female	Start day 0/end day 7 (max grade 2)	Fever, hypotension (grade 2)	Start day 5/end day 11 (max grade 3)	Lethargy (awake on physical stimulation only)	Tocilizumab, Dexamethasone, Anakinra
9	64, female	Start day 10/end day 13 (max grade 2)	Fever, hypotension (grade 2)			Tocilizumab
10	54, male	Start day 3/end day 4 (max grade 1)	Fever			Tocilizumab
11	57, female	Start day 4/end day 6 (max grade 1)	Fever			Tocilizumab
12	41, male	Start day 1/end day 6 (max grade 1)	Fever	Start day 5/end day 7 (max grade 3)	Lethargy (awake on verbal stimulation only); convulsion	Tocilizumab, Dexamethasone, Anakinra
13	66, male	Start day 1/end day 6 (max grade 1)	Fever			None
14	51, male	Start day 2/end day 6 (max grade 2)	Fever, hypoxia (grade 2)			None
15	44, female	Start day 1/end day 21 (max grade 4)	Fever, hypotension (grade 4), hypoxia (grade 4)	Start day 2/end day 22 (max grade 3)	Lethargy (awake on physical stimulation only)	Tocilizumab, Dexamethasone, Anakinra, CRRT
16	69, male	Start day 5/end day 8 (max grade 2)	Fever, hypotension (grade 2), hypoxia (grade 2)	Start day 8/end day 9 (max grade 1)	Orientation deficit	Tocilizumab

Note: Toxicity grades are as follows: grade 0, no toxicity; grade 1, mild toxicity; grade 2, moderate toxicity; grade 3, severe toxicity; grade 4, life-threatening toxicity; grade 5, death.

Abbreviations: CRRT, continuous renal replacement therapy; CRS, cytokine release syndrome; ICANS, immune effector cell-associated neurotoxicity; Pt, patient.

patients with controls at a single-patient level and within each other at a group level. Two-sample *T*-test design in SPM12 was used for all analyses including age and sex as nuisances. Treatment of CRS or ICANS (namely, tocilizumab with or without corticosteroids) was also included as a potential confounding variable in the analysis. A family-wise error (FWE)-corrected height threshold <.05 both at peak and cluster levels was initially considered significant. Then, a *p*-value of <.001 uncorrected at peak level with an FWE-correction <.05 at cluster level was also considered to minimize type II errors and for a wider exploration of metabolic correlates of CRS and ICANS at a single patient's level.[36] Only clusters with size $k \geq 100$ voxels were considered. The *t*-student test was used to compare MTV and TLG between patients with CRS with or without ICANS.

RESULTS

Patients' characteristics

A total of 26 patients were treated with CAR T at IRCCS Ospedale Policlinico San Martino between October 2020 and November 2022. After treatment with CAR T, 13 patients experienced CRS without ICANS

JOURNAL OF NEUROIMAGING
THE OFFICIAL JOURNAL OF THE AMERICAN SOCIETY OF NEUROIMAGING

TABLE 3 Brain regions of hypometabolism in patients with ICANS after treatment with CAR-T.

	Cluster level		Peak level					
Cluster extent	Corrected *p* value	Cortical region	Maximum *Z* score		Talairach coordinates		Cortical region	BA
2058	.001							
		L-Frontal	5.9	−10	14	−52	Superior frontal gyrus	6
		R-Frontal	5.8	52	20	2	Inferior frontal gyrus	47
		R-Frontal	5.7	45	44	−10	Middle frontal gyrus	11
		R-Frontal	5.35	35	52	−12	Superior frontal gyrus	11
		L-Frontal	5.21	−22	26	36	Middle frontal gyrus	9
		R-Limbic	5.00	12	36	24	Anterior cingulate gyrus	32
		R-Temporal	4.67	66	−2	12	Middle temporal gyrus	21
		R-Occipital	4.10	54	−68	10	Middle occipital gyrus	19
		L-Parietal	3.89	−38	−30	42	Inferior parietal gyrus	40

Note: A *p*-value of <.05 family-wise error-corrected both at peak and at cluster levels was accepted as statistically significant. In the "cluster level" section on the left, the corrected *p*-value and the brain lobe with hypometabolism are reported. In the "peak level" section on the right, the *Z* score and peak coordinates and the corresponding cortical region and Brodmann area (BA) are reported.
Abbreviations: ICANS, immune effector cell-associated neurotoxicity; L, left; R, right.

(CRS group), 6 patients experienced CRS and ICANS (ICANS group), while 11 patients did not show CAR T-related toxicities (no-toxicity). Based on the above-described exclusion criteria, 5 out of 26 patients were excluded from the present analyses. In fact, FDG-PET could not be performed 30 days after treatment in 4 patients for clinical reasons (1 CRS, 1 ICANS, and 2 no-toxicity patients), while in 1 patient who later developed CRS, baseline brain MRI and [^{18}F]FDG PET were already showing postradiation changes in the cerebellum due to a previous treatment. No patients were excluded due to the presence of acute ischemia or hemorrhage on their MRI scans. Twenty-one patients were thus finally analyzed and compared with the 21 controls. Clinical data of these 21 patients (11 CRS, 5 ICANS, 5 not-toxicity) are detailed in Table 1. Table 2 provides further details on the timeframe of onset and clinical manifestations in patients with CRS with and without ICANS. All patients who experienced ICANS received Tocilizumab, Dexamethasone, and Anakinra except one showing ICANS grade 4 who received Tocilizumab only (as the majority of patients with CRS, see Table 2). One patient also underwent continuous renal replacement therapy.

Metabolic correlates of ICANS and CRS

No significant common patterns of hypometabolism with respect to controls were highlighted in all subgroups at baseline (before therapy with CAR-T). Thirty days after therapy, ICANS group showed an extended and bilateral pattern of hypometabolism with respect to controls mainly involving the orbitofrontal cortex, frontal dorsolateral cortex, anterior cingulate, temporolateral cortex bilaterally, and two smaller clusters located in the right middle occipital gyrus and left, inferior parietal lobule, respectively (FWE-corrected $p < .003$; see Figure 1; Table 3). By contrast in ICANS, MRI findings were unrevealing or showed only sparse T2/FLAIR hyperintensities throughout the white matter (unchanged with respect to baseline). Similarly, electroencephalogram (EEG) findings were rather unspecific in these patients as they showed diffuse slowing of the brain electrical activity in line with a metabolic encephalopathy except for one case where the EEG showed epileptiform abnormalities.

On the other side, patients who experienced CRS without ICANS showed significant hypometabolism in less extended clusters mainly involving bilateral medial and lateral temporal lobes, posterior parietal lobes, anterior cingulate, and cerebellum (FWE-corrected $p < .002$; Figure 2; Table 4).

When ICANS and CRS subgroups were directly compared, patients with ICANS showed a significantly more prominent hypometabolism in the orbitofrontal and frontal dorsolateral cortex in both hemispheres (FWE-corrected $p < .002$; Figure 3). Indeed, also in the single-patient analyses, significant clusters of frontal hypometabolism were evident in all ICANS patients, while patients who experienced CRS without ICANS showed small and topographically heterogeneous clusters of hypometabolism (Figures 4 and 5). Three CRS patients did not show significant regions of hypometabolism with respect to controls. Similarly, no significant common patterns of hypometabolism were highlighted at PET-30 in the no-toxicity subgroup.

MTV and TLG and CAR T-related toxicity

As shown in Figure 6, the mean baseline MTV was 251 (range: 92-514) cm^3 in ICANS and 65 (range: 18-234) cm^3 in CRS subgroups, resulting significantly higher in the former group ($p < .02$).

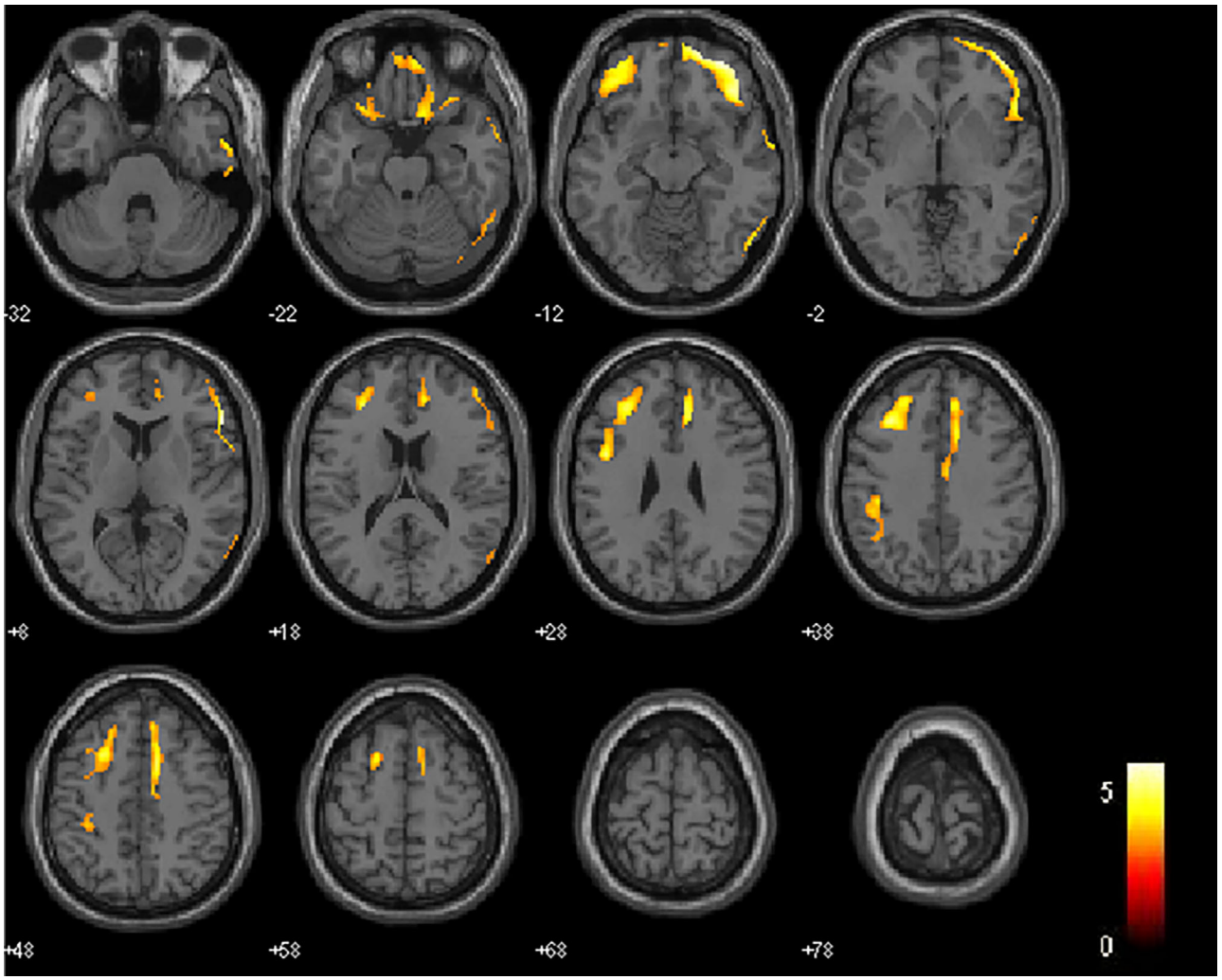

FIGURE 1 Regions of relative hypometabolism in patients with cytokine release syndrome evolved to immune-effector cell-associated neurotoxicity syndrome (ICANS) with respect to controls. ICANS group showed a bilateral pattern of hypometabolism mainly involving the orbitofrontal cortex, frontal dorsolateral cortex, anterior cingulate, temporolateral cortex bilaterally, and two smaller clusters located in the right middle occipital gyrus and left, inferior parietal lobule, respectively (family-wise error-corrected $p < .003$). Clusters with significant hypometabolism are shown superimposed on an MRI template. The color bar indicates the level of *z*-scores for significant voxels (yellow: highest; red: lowest; see Table 3 for details on coordinates and *Z*-scores).

TABLE 4 Brain regions of hypometabolism in CRS patients after treatment with CAR-T.

	Cluster level		Peak level					
Cluster extent	Corrected *p* value	Cortical region	Maximum Z score		Talairach coordinates		Cortical region	BA
2058	.001							
		R-Temporal	4.67	48	−28	−16	Fusiform gyrus	20
		R-Limbic	4.67	45	−20	−12	Parahippocampal gyrus	20
		L-Temporal	4.67	−36	2	−34	Middle temporal gyrus	21
		R-Cerebellum	4.67	18	−72	−4	Inferior semilunar lobule	
		R-Cerebellum	4.67	10	−46	−36	Cerebellar tonsil	

Note: A *p*-value of <.05 family-wise error-corrected both at peak and at cluster levels was accepted as statistically significant. In the "cluster level" section on the left, the corrected *p* value and the brain lobe with hypometabolism are reported. In the "peak level" section on the right, the *Z* score and peak coordinates and the corresponding cortical region and Brodmann area (BA) are reported.
Abbreviations: CRS, cytokine release syndrome; L, left; R, right.

JOURNAL OF NEUROIMAGING
THE OFFICIAL JOURNAL OF THE AMERICAN SOCIETY OF NEUROIMAGING

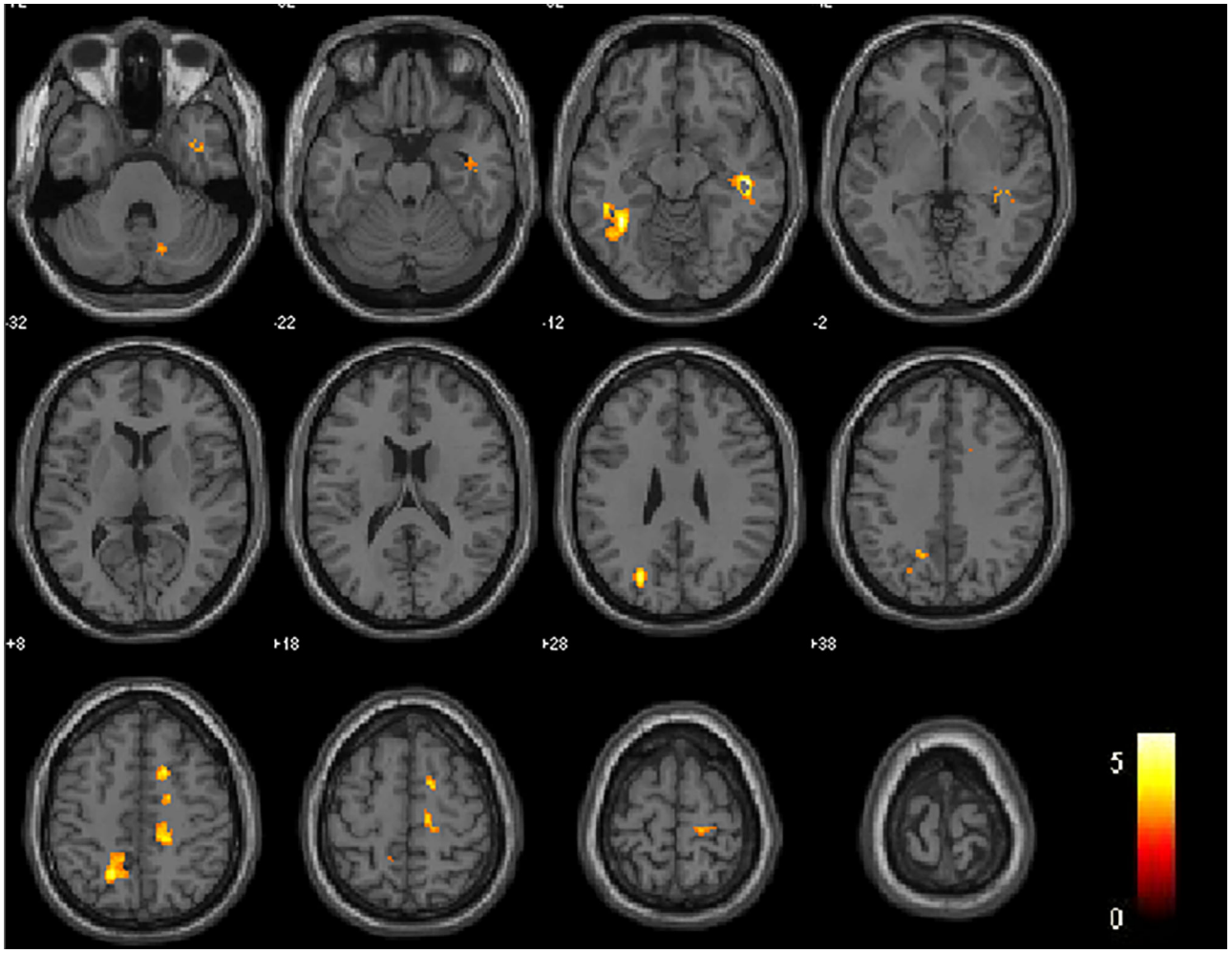

FIGURE 2 Regions of relative hypometabolism in patients with cytokine release syndrome with respect to controls. Patients who experienced cytokine release syndrome without immune-effector cell-associated neurotoxicity syndrome showed significant hypometabolism in less extended clusters mainly involving bilateral medial and lateral temporal lobes, posterior parietal lobes, anterior cingulate, and cerebellum (family-wise error-corrected $p < .002$). Clusters with significant hypometabolism are shown superimposed on an MRI template. The color bar indicates the level of *Z*-scores for significant voxels (yellow: highest; red: lowest; see Table 4 for details on coordinates and *Z*-scores).

Similarly, TLG was significantly higher (1810, range SUV mean × cm^3) in ICANS with respect to CRS subgroup (425, range SUV mean × cm^3, $p < .01$).

DISCUSSION

This is the first group analysis specifically targeting brain PET functional correlates of CRS and ICANS in DLBCL patients treated with CAR-T. Patients with CRS either associated or not with ICANS showed regions of hypometabolism with respect to controls; however, voxel-based analyses demonstrated a more extended and prominent involvement of the frontolateral cortex in patients who evolved to ICANS. This pattern was highlighted in all patients with ICANS also at a single patient's level and is in keeping with the pathophysiological hypothesis of ICANS as a predominant frontal syndrome.[29,37]

In previously published case series, clinical features of ICANS have more often been discussed with respect to patients' MRI findings.[9,15,38] Actually, many patients with ICANS have a negative MRI, and typical MRI features of ICANS have not yet been defined.[38] However, multifocal microhemorrhages, extensive cortical diffusion restriction due to cytotoxic edema, leptomeningeal enhancement, and diffusion restriction in the corpus callosum have been previously reported in some ICANS patients.[8,9,39] It should be noted that, at least some of these MRI findings, when present, can also be reflected as an alteration in brain metabolism at [^{18}F]FDG PET, thus complicating the pathophysiological interpretation of [^{18}F]FDG PET patterns in such scenarios. For this reason, only ICANS patients with negative or unspecific MRI results were included in the present study. Accordingly, the pattern of hypometabolism highlighted in patients with ICANS is expected to reflect more directly the impairment of metabolic/functional networks.

In this regard, the presence of an extended frontal hypometabolism is in keeping with the hypothesis of frontal dysfunctions, already

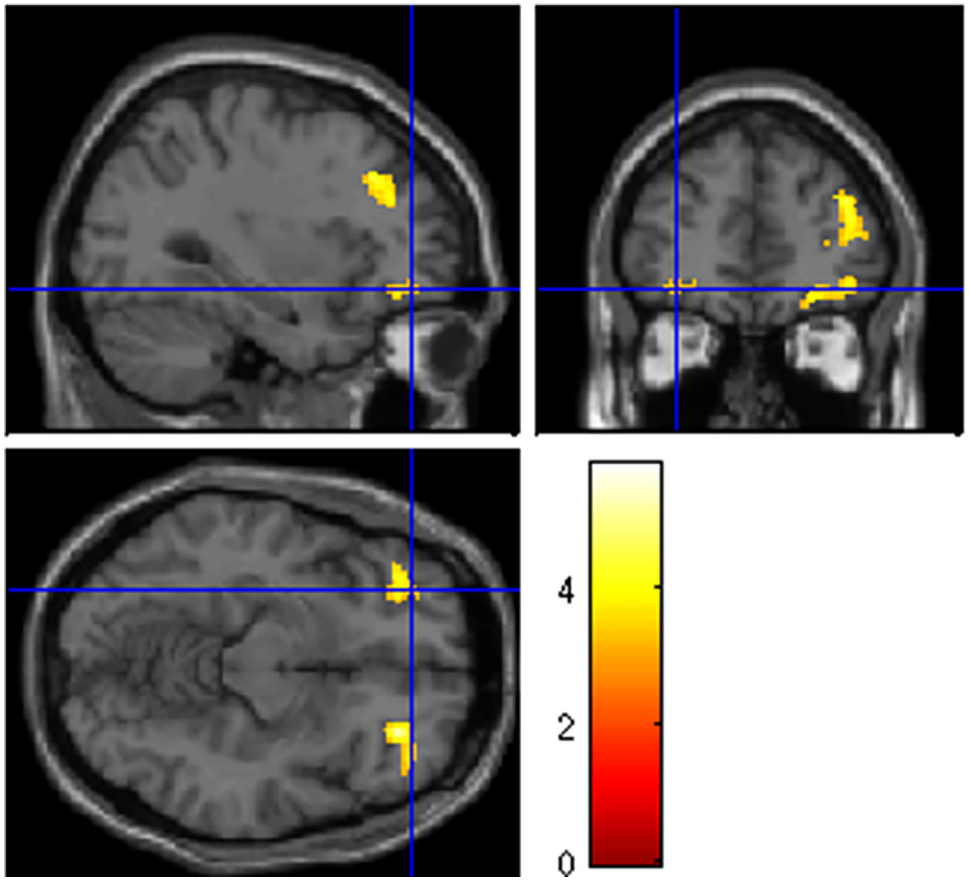

FIGURE 3 Regions of relative hypometabolism in patients with cytokine release syndrome (CRS) and immune-effector cell-associated neurotoxicity syndrome (ICANS) with respect to patients with CRS only. When ICANS and CRS subgroups were directly compared, patients with ICANS showed a significantly more prominent hypometabolism in the orbitofrontal and frontal dorsolateral cortex in both hemispheres (family-wise error-corrected $p < .002$). Clusters with significant hypometabolism are shown superimposed on an MRI template. The color bar indicates the level of *Z*-scores for significant voxels (yellow: highest; red: lowest).

proposed in the few available case reports or case series including FDG-PET in ICANS patients. Indeed, the most common EEG pattern reported in patients with ICANS is a diffuse slowing and a frontal intermittent rhythmic delta activity consistent with encephalopathy.[8,9,39] Similarly, clinical features of ICANS include ideomotor and fluency slowing, akinetic mutism, dyscalculia, and writing disorders such as reiterative writing behaviors.[29] All these symptoms can be related to frontal (or frontal-subcortical) dysfunction.

Notably, one of the patients with ICANS included in the present study developed an orientation deficit. This patient showed hypometabolism involving the bilateral dorsolateral prefrontal cortex. As a matter of fact, normal functioning of the attentional orienting system is critical for effective behavior and it has been previously demonstrated that the dorsolateral prefrontal cortex plays an important role in exogenous orienting.[40,41] In all the other patients included in this study, ICANS was associated with lethargy and patients could be awakened after verbal or physical stimulation only.

It is well-known that systemic inflammation can impact brain function, resulting in lethargy and related impaired cognitive abilities.[42] The link between systemic inflammation and frontal cortex function has been previously investigated in preclinical models.[43] These previous studies demonstrated that frontal lobes are most susceptible to cytokine-induced inflammation potentially, explaining the frontal-predominant dysfunction observed in disorders associated with severe systemic inflammation.[43] In particular, preclinical studies demonstrated that frontal lobes have the greatest inflammatory response following tumor necrosis factor-alpha (TNF-α) stimulation.[43]

In recent years, clinical and imaging features of encephalopathies related to systemic inflammation and cytokine storm disorders have been extensively reviewed especially in the framework of encephalopathy associated with the coronavirus disease 2019 (COVID-19).[10,44–47] Indeed electroclinical frontal lobe dysfunction has been reported[10,48] in neurocovid patients and cytokine-mediated neuroinflammation has been proposed as a common mechanism resulting in encephalopathy in the framework of many systemic inflammations.

The average lower serum cytokine load detected in COVID-19-associated cytokine storm (compared with other CRSs) has been advocated to explain the lower incidence of encephalopathy in COVID-19 with respect to other inflammatory syndromes.[10]

A similar mechanism could underlie, in our patients, the different evolution of CRS (with or without ICANS) as well as the lower topographical consistency of hypometabolic pattern in patients with CRS

JOURNAL OF NEUROIMAGING
THE OFFICIAL JOURNAL OF THE AMERICAN SOCIETY OF NEUROIMAGING
WILEY

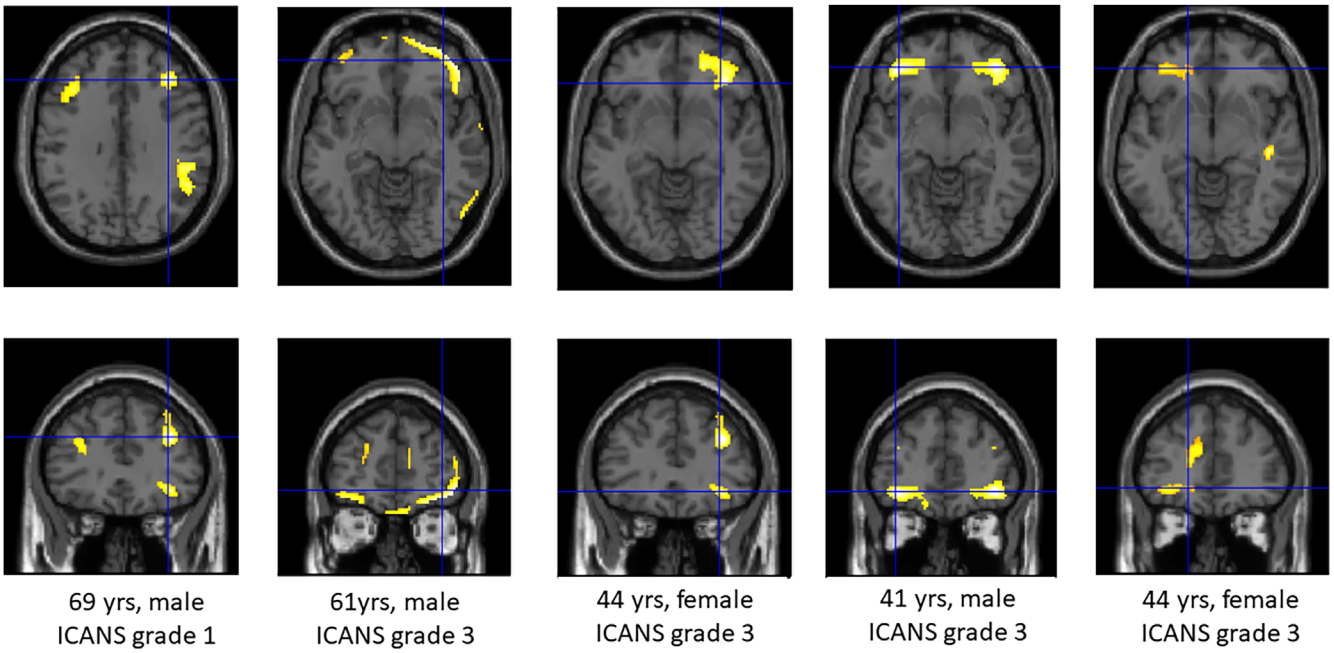

FIGURE 4 Results of voxel-based single-subject analyses for the comparison of brain metabolism between patients with immune-effector cell-associated neurotoxicity syndrome (ICANS) and control. A *p*-value of <.001 was accepted as significant for the single-subject analyses. Clusters with significant hypometabolism are shown superimposed on an MRI template. The color bar indicates the level of *Z*-scores for significant voxels (yellow: highest; red: lowest). yrs, years.

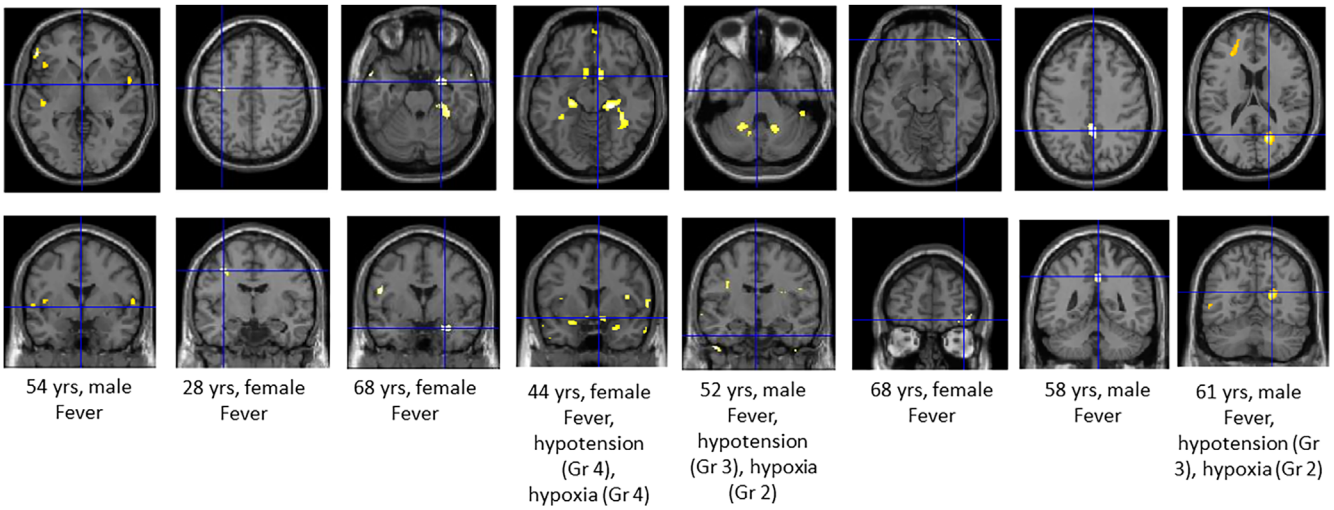

FIGURE 5 Single subject analyses comparing brain metabolism in cytokine release syndrome patients with respect to controls. A *p*-value of <.001 was accepted as significant for the single-subject analyses. Clusters with significant hypometabolism are shown superimposed on an MRI template. Gr, grades (grade 1: mild toxicity; grade 3: severe toxicity); MTV, metabolic tumor volume; TLG, total lesion glycolysis; yrs, years.

(with respect to what is highlighted in patients with both CRS and ICANS). In fact, an added value of the present study is the specific evaluation of brain metabolism also in CRS patients who have not experienced ICANS. These patients showed sparser (and smaller) clusters of hypometabolism with a generally less prominent involvement of the frontal cortex. This less extended pattern of hypometabolism is also in keeping with the capability of FDG-PET to mirror disease severity in neurocognitive disorders.

In the present proof of concept analysis, we did not measure cytokine levels. However, a different intensity regarding cytokine release between CRS patients with or without ICANS can be hypothesized based on the greater metabolic tumor burden in CRS patients who evolved to ICANS. In this regard, it has been previously suggested that patients with higher baseline tumor burden have a significantly increased risk of severe CRS due to a higher cytokine release.[48] In our analysis, all ICANS patients had an MTV >90 cm^3 and the patient

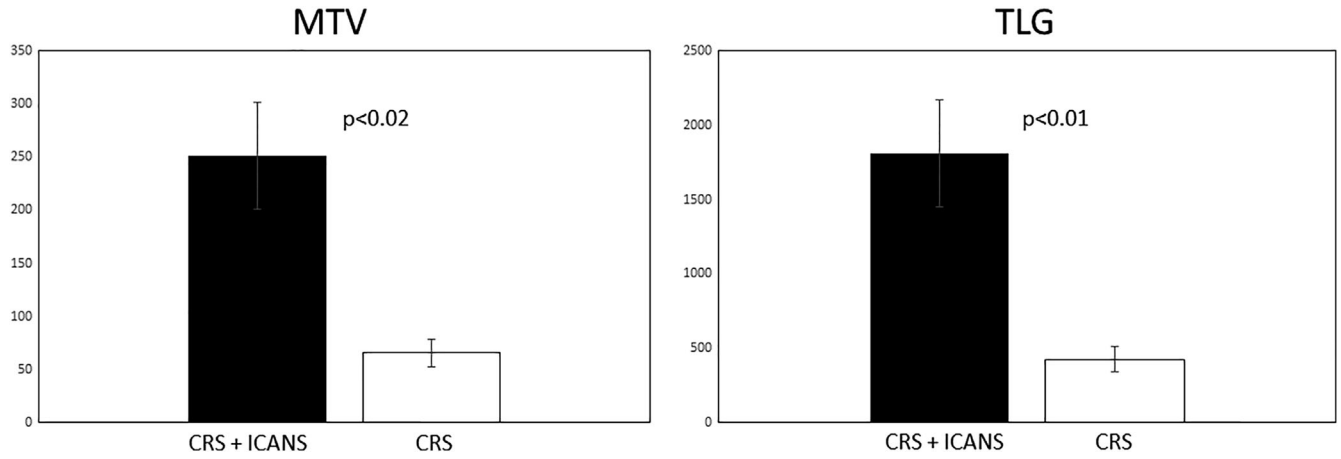

FIGURE 6 Baseline metabolic tumor volume and total lesion glycolysis in patients who developed cytokine release syndrome only and in patients who developed cytokine release syndrome and immune-effector cell-associated neurotoxicity syndrome. CRS, cytokine release syndrome; ICANS, immune-effector cell-associated neurotoxicity; MTV, metabolic tumor volume; TLG, total lesion glycolysis.

with the highest MTV showed ICANS grade 3 with marked lethargy (responsive physical stimulation only) together with fever, grade 4 hypotension, and hypoxia and was the only one requiring continuous renal replacement therapy.

It should be noted, however, that the link between high tumor burden and the specific development of ICANS has not yet been clearly proven (and probably requires a detailed investigation in different disease settings and based on the different types of CAR T-cell therapy). Regardless of the relationship between patients' MTV and the occurrence of ICANS, the evidence of frontal hypometabolism in the present group of patients might further support the role of cytokine release in ICANS pathophysiology. In this regard, Hong and colleagues demonstrated a strong correlation between TLG and the peak value of IL-6, interferon gamma, and ferritin.[49] Similarly, in a study targeting murine brain inflammation, Young et al. showed that after exposure to TNF-α, frontal and temporal cortical regions are characterized by a 10-fold greater upregulation of nuclear factor kappa-light-chain-enhancer of activated B cells with respect to the cerebellum.

This study has limitations. First, a larger number of patients would be needed to further address this relevant issue, thus translating this preliminary evidence into the risk stratification of patients with respect to inflammatory side effects of CAR-T. Similarly, we acquired brain [^{18}F]FDG PET 30 days after treatment as part of the first posttherapy assessment. However, the onset and resolution of ICANS and CRS occurred earlier than 30 days in all the studied patients. The choice to acquire brain [^{18}F]FDG PET in the framework of PET-30 was mainly due to the explorative nature of the present analysis and to radioprotection issues. However, the definition of disease patterns still evident 30 days after therapy may allow inferring preliminary pathophysiology hypothesis, thus guiding more clinically oriented imaging studies targeting inflammatory toxicity of CAR-T. One further limitation of this study is that bridging therapy was differently administered in this group of patients. This heterogeneity prevents us to propose further hypotheses on risk factors for ICANS and CRS. However, the lack of common hypometabolic patterns in subgroups of patients at baseline seems to suggest that preconditioning may not be a strong determinant for the generation of the final hypometabolic pattern. Finally, some patients with ICANS were treated with corticosteroids and thus this variable was added as a nuisance in the SPM analysis. It should be noted, however, that while corticosteroids might indirectly affect brain FDG-PET scan quality (due to their effect on patients' glucose levels), no regional effect is expected at cortical levels.[31]

In conclusion, this group of patients with ICANS after treatment with CAR-T was characterized by high metabolic tumor burden (a potential risk factor for a greater cytokine release) and showed a frontolateral hypometabolic signature in line with the hypothesized more prominent susceptibility of frontal lobes to cytokine-induced inflammation. These preliminary results may encourage a more systematic investigation of the role of [^{18}F]FDG PET in the clinical and pathophysiologic assessment of CAR-T-related neurotoxicity.

ACKNOWLEDGMENTS

The authors have nothing to report.

CONFLICT OF INTEREST STATEMENT

SM received speaker honoraria from G.E. Healthcare and Life Molecular Imaging and honoraria for participation in advisory boards from Eli-Lilly. MB has received speaker honoraria from G.E. Healthcare. MI serves as an Editorial Board member of Multiple Sclerosis and received honoraria for participation in advisory boards from Biogen, BMS, Novartis, Merck, Janssen, Sanofi, and Roche. EA received honoraria for participation in advisory boards from Novartis, BlueBirdBio, Regeneron, GILEAD-KITE, and Sanofi; for data monitoring committee from BSM (Celgene), Vifor Pharma, and Vertex; and for consultation from Menarini-stemline. All the other authors declare no conflicts of interests.

ORCID

Matteo Bauckneht hiips://orcid.org/0000-0002-1937-9116

REFERENCES

1. Neelapu SS, Locke FL, Bartlett NL, et al. Axicabtagene ciloleucel CAR T-cell therapy in refractory large B-cell lymphoma. N Engl J Med. 2017;377:2531–44.
2. Crump M, Neelapu SS, Farooq U, et al. Outcomes in refractory diffuse large B-cell lymphoma: results from the international SCHOLAR-1 study. Blood. 2017;130:1800–8.
3. Gutierrez C, McEvoy C, Mead E, et al. Management of the critically ill adult chimeric antigen receptor-T cell therapy patient: a critical care perspective. Crit Care Med. 2018;46:1402–10.
4. Brudno JN, Kochenderfer JN. Chimeric antigen receptor T-cell therapies for lymphoma. Nat Rev Clin Oncol. 2018;15:31–46.
5. Jiang H, Liu L, Guo T, et al. Improving the safety of CAR-T cell therapy by controlling CRS-related coagulopathy. Ann Hematol. 2019;98:1721–32.
6. Fitzgerald JC, Weiss SL, Maude SL, et al. Cytokine release syndrome after chimeric antigen receptor T cell therapy for acute lymphoblastic leukemia. Crit Care Med. 2017;45:e124–31.
7. Teachey DT, Lacey SF, Shaw PA, et al. Identification of predictive biomarkers for cytokine release syndrome after chimeric antigen receptor T-cell therapy for acute lymphoblastic leukemia. Cancer Discov. 2016;6:664–79.
8. Santomasso BD, Park JH, Salloum D, et al. Clinical and biological correlates of neurotoxicity associated with CAR T-cell therapy in patients with B-cell acute lymphoblastic leukemia. Cancer Discov. 2018;8:958–71.
9. Rubin DB, Danish HH, Ali AB, et al. Neurological toxicities associated with chimeric antigen receptor T-cell therapy. Brain. 2019;142:1334–8.
10. Pensato U, Muccioli L, Cani I, et al. Brain dysfunction in COVID-19 and CAR-T therapy: cytokine storm-associated encephalopathy. Ann Clin Transl Neurol. 2021;8:968–79.
11. Pensato U, Guarino M, Muccioli L. The role of neurologists in the era of cancer immunotherapy: focus on CAR T-cell therapy and immune checkpoint inhibitors. Front Neurol. 2022;13:936141.
12. Lee DW, Santomasso BD, Locke FL, et al. ASTCT consensus grading for cytokine release syndrome and neurologic toxicity associated with immune effector cells. Biol Blood Marrow Transplant. 2019;25:625–38.
13. Gofshteyn JS, Shaw PA, Teachey DT, et al. Neurotoxicity after CTL019 in a pediatric and young adult cohort. Ann Neurol. 2018;84:537–46.
14. Sokolov E, Karschnia P, Benjamin R, et al. Language dysfunction-associated EEG findings in patients with CAR-T related neurotoxicity. BMJ Neurol Open. 2020;2:e000054.
15. Strati P, Nastoupil LJ, Westin J, et al. Clinical and radiologic correlates of neurotoxicity after axicabtagene ciloleucel in large B-cell lymphoma. Blood Adv. 2020;4:3943–51.
16. Gust J, Hay KA, Hanafi L-A, et al. Endothelial activation and blood–brain barrier disruption in neurotoxicity after adoptive immunotherapy with CD19 CAR-T cells. Cancer Discov. 2017;7:1404–19.
17. Sjöholm T, Korenyushkin A, Gammelgård G, et al. Whole body FDG PET/MR for progression free and overall survival prediction in patients with relapsed/refractory large B-cell lymphomas undergoing CAR T-cell therapy. Cancer Imaging. 2022;22:76.
18. Guidetti A, Dodero A, Lorenzoni A, et al. Combination of Deauville score and quantitative positron emission tomography parameters as a predictive tool of anti-CD19 chimeric antigen receptor T-cell efficacy. Cancer. 2023;129:255–63.
19. Galtier J, Vercellino L, Chartier L, et al. Positron emission tomography-imaging assessment for guiding strategy in patients with relapsed/refractory large B-cell lymphoma receiving CAR T cells. Haematologica. 2023;108:171–80.
20. Breen WG, Hathcock MA, Young JR, et al. Metabolic characteristics and prognostic differentiation of aggressive lymphoma using one-month post-CAR-T FDG PET/CT. J Hematol Oncol. 2022;15:36.
21. Cohen D, Beyar-Katz O, Even-Sapir E, et al. Lymphoma pseudoprogression observed on [18F]FDG PET-CT scan 15 days after CAR-T infusion. Eur J Nucl Med Mol Imaging. 2022;49:2447–9.
22. Al Zaki A, Feng L, Watson G, et al. Day 30 SUVmax predicts progression in patients with lymphoma achieving PR/SD after CAR T-cell therapy. Blood Adv. 2022;6:2867–71.
23. Cohen D, Luttwak E, Beyar-Katz O, et al. [18F]FDG PET-CT in patients with DLBCL treated with CAR-T cell therapy: a practical approach of reporting pre- and post-treatment studies. Eur J Nucl Med Mol Imaging. 2022;49:953–62.
24. Dean EA, Mhaskar RS, Lu H, et al. High metabolic tumor volume is associated with decreased efficacy of axicabtagene ciloleucel in large B-cell lymphoma. Blood Adv. 2020;4:3268–76.
25. Wang J, Hu Y, Yang S, et al. Role of fluorodeoxyglucose positron emission tomography/computed tomography in predicting the adverse effects of chimeric antigen receptor T cell therapy in patients with non-Hodgkin lymphoma. Biol Blood Marrow Transplant. 2019;25:1092–8.
26. Hong R, Tan Su Yin E, Wang L, et al. Tumor burden measured by 18F-FDG PET/CT in predicting efficacy and adverse effects of chimeric antigen receptor T-Cell therapy in non-Hodgkin lymphoma. Front Oncol. 2021;11:713577.
27. Paccagnella A, Farolfi A, Casadei B, et al. 2-[18F]FDG-PET/CT for early response and brain metabolic pattern assessment after CAR-T cell therapy in a diffuse large B cell lymphoma patient with ICANS. Eur J Nucl Med Mol Imaging. 2022;49:1090–1.
28. Beuchat I, Danish HH, Rubin DB, et al. EEG findings in CAR T-cell-associated neurotoxicity: clinical and radiological correlations. Neuro Oncol. 2022;24:313–25.
29. Pensato U, Amore G, D'Angelo R, et al. Frontal predominant encephalopathy with early paligraphia as a distinctive signature of CAR T-cell therapy-related neurotoxicity. J Neurol. 2022;269:609–15.
30. Boellaard R, Delgado-Bolton R, Oyen WJ, et al. FDG PET/CT: EANM procedure guidelines for tumour imaging: version 2.0. Eur J Nucl Med Mol Imaging. 2015;42:328–54.
31. Guedj E, Varrone A, Boellaard R, et al. EANM procedure guidelines for brain PET imaging using [18F]FDG, version 3. Eur J Nucl Med Mol Imaging. 2022;49:632–51.
32. Friston KJ, Holmes AP, Worsley KJ, et al. Statistical parametric maps in functional imaging: a general linear approach. Hum Brain Mapp. 1994;2:189–210.
33. Morbelli S, Piccardo A, Villavecchia G, et al. Mapping brain morphological and functional conversion patterns in amnestic MCI: a voxel-based MRI and FDG-PET study. Eur J Nucl Med Mol Imaging. 2010;37:36–45.
34. Kruse V, Mees G, Maes A, et al. Reproducibility of FDG PET based metabolic tumor volume measurements and of their FDG distribution within. Q J Nucl Med Mol Imaging. 2015;59:462–8.
35. Morbelli S, Bauckneht M, Arnaldi D, et al. 18F-FDG PET diagnostic and prognostic patterns do not overlap in Alzheimer's disease (AD) patients at the mild cognitive impairment (MCI) stage. Eur J Nucl Med Mol Imaging. 2017;44:2073–83.
36. Lieberman MD, Cunningham WA. Type I and type II error concerns in fMRI research: re-balancing the scale. Soc Cogn Affect Neurosci. 2009;4:423–8.
37. Pensato U, Amore G, Muccioli L, et al. CAR t-cell therapy in BOlogNa-NEUrotoxicity TReatment and Assessment in Lymphoma (CARBONNEUTRAL): proposed protocol and results from an Italian study. J Neurol. 2023;270:2659–73.

38. Smith DA, Kikano E, Tirumani SH, et al. Imaging-based toxicity and response pattern assessment following CAR T-cell therapy. Radiology. 2022;302:438–45.
39. Rice J, Nagle S, Randall J, et al. Chimeric antigen receptor T cell-related neurotoxicity: mechanisms, clinical presentation, and approach to treatment. Curr Treat Options Neurol. 2019;21:40.
40. Snyder JJ, Chatterjee A. The frontal cortex and exogenous attentional orienting. J Cogn Neurosci. 2006;18:1913–23.
41. Takahashi M, Ikegami M. Differential frontal activation during exogenous and endogenous orientation of visuospatial attention. A near-infrared spectroscopy study. Neuropsychobiology. 2008;58:55–64.
42. Odoj K, Brawek B, Asavapanumas N, et al. In vivo mechanisms of cortical network dysfunction induced by systemic inflammation. Brain Behav Immun. 2021;96:113–26.
43. Young AM, Campbell EC, Lynch S, et al. Regional susceptibility to TNF-α induction of murine brain inflammation via classical IKK/NF-κB signalling. PLoS One. 2012;7:e39049.
44. Perrin P, Collongues N, Baloglu S, et al. Cytokine release syndrome-associated encephalopathy in patients with COVID-19. Eur J Neurol. 2021;28:248–58.
45. Guedj E, Million M, Dudouet P, et al. 18F-FDG brain PET hypometabolism in post-SARS-CoV-2 infection: substrate for persistent/delayed disorders? Eur J Nucl Med Mol Imaging. 2021;48:592–95.
46. Guedj E, Morbelli S, Kaphan E, et al. From early limbic inflammation to long COVID sequelae. Brain. 2021;144:e65.
47. Pilotto A, Masciocchi S. SARS-CoV-2 encephalitis is a cytokine release syndrome: evidences from cerebrospinal fluid analyses. Clin Infect Dis. 2021;73:e3019–26.
48. Muccioli L, Pensato U, Cani I, et al. COVID-19-associated encephalopathy and cytokine-mediated neuroinflammation. Ann Neurol. 2020;88:860–1.
49. Hong R, Tan Su Yin E, Wang L, et al. Tumor burden measured by 18F-FDG PET/CT in predicting efficacy and adverse effects of chimeric antigen receptor T-cell therapy in non-Hodgkin lymphoma. Front Oncol. 2021;11:713577.

How to cite this article: Morbelli S, Gambella M, Raiola AM, Ghiggi C, Bauckneht M, Raimondo TD, et al. Brain FDG-PET findings in chimeric antigen receptor T-cell therapy neurotoxicity for diffuse large B-cell lymphoma. J Neuroimaging. 2023;1–12. hiips://doi.org/10.1111/jon.13135